COMPUTATIONAL PHYSICS | JANUARY 01 2020

Conservative numerical methods for nonlinear oscillators

Mark H. Holmes

Am. J. Phys. 88, 60–69 (2020)
https://doi.org/10.1119/10.0000295

COMPUTATIONAL PHYSICS

The Computational Physics Section publishes articles that help students and their instructors learn about the physics and the computational tools used in contemporary research. Most articles will be solicited, but interested authors should email a proposal to the editors of the Section, Jan Tobochnik (jant@kzoo.edu) or Harvey Gould (hgould@clarku.edu). Summarize the physics and the algorithm you wish to include in your submission and how the material would be accessible to advanced undergraduates or beginning graduate students.

Conservative numerical methods for nonlinear oscillators

Mark H. Holmes
Department of Mathematical Sciences, Rensselaer Polytechnic Institute, Troy, New York 12180-3590

(Received 18 July 2019; accepted 25 August 2019)

I show that it is straightforward to derive numerical methods that conserve the energy of nonlinear oscillators. The derivation is first done for a single particle and then extended to multiple particle systems. Examples considered include the pendulum, the Hénon-Heiles model, and the Fermi-Pasta-Ulam problem. Numerical experiments are shown and comparisons are made with nonconservative methods.
https://doi.org/10.1119/10.0000295

I. INTRODUCTION

One of the more important properties a system can possess is conservation of energy. Although there has been considerable effort to derive numerical methods that preserve this property, progress has been uneven. As an example, after finding that standard numerical methods are capable of conserving energy only after making several questionable *ad hoc* modifications, one author concluded that maybe "energy-conserving schemes do not necessarily capture all relevant qualitative features" of the problem.[1] Nevertheless, conservative methods have been found, the most well-known of which are discrete variable methods and the average vector field method.[2–6] Although the first energy conserving methods were derived almost 40 years ago, most computational physics textbooks have little, if any, discussion of them or conservative methods in general.

The purpose of this paper is to show that it is fairly simple to derive conservative methods and to provide a derivation for examples often considered in introductory mechanics and dynamics courses. These methods will be compared to symplectic methods,[6–8] as well as more general purpose solvers. For a fixed time step, symplectic methods typically do not conserve the energy,[9,10] but can provide an approximate solution that is close to being conservative over a very long time interval.[6] There are adaptive methods that are both conservative and symplectic, but they will not be considered here.[11]

II. BACKGROUND

We start by considering the single particle problem of solving $m\ddot{y}(t) = F(y)$, where $y(0) = a$ and $\dot{y}(0) = b$. These equations can be rewritten as

$$\dot{y} = v(t), \tag{1}$$

$$m\dot{v}(t) = F(y). \tag{2}$$

Single step numerical methods used to solve this problem have the form

$$y_{n+1} = y_n + \tilde{v}\Delta t, \tag{3}$$

$$v_{n+1} = v_n + \frac{\Delta t}{m}\tilde{F}, \tag{4}$$

where $y_n \equiv y(t)$, $y_{n+1} \equiv y(t+\Delta t)$, $v_n \equiv v(t)$, and $v_{n+1} \equiv v(t+\Delta t)$. The choice of the transitional velocity $\tilde{v}$ and transitional force $\tilde{F}$ depends on the method. As an example, the average of two time steps is taken for the trapezoidal method, and $\tilde{v} = (v_{n+1} + v_n)/2$ and $\tilde{F} = [F(y_{n+1}) + F(y_n)]/2$. For brevity of notation, we will write $F_n \equiv F(y_n, v_n)$ and $F_{n+1} \equiv F(y_{n+1}, v_{n+1})$ in the following.

Even for a linear force for which $F(y) = -\alpha y$, most methods are not conservative. One exception is the trapezoidal method. To show this property, note that the current value of the energy is $H_n \equiv H(y_n, v_n) = mv_n^2/2 + \alpha y_n^2/2$, and its value at the next time step is $H_{n+1} \equiv H(y_{n+1}, v_{n+1}) = mv_{n+1}^2/2 + \alpha y_{n+1}^2/2$. Therefore,

$$H_{n+1} - H_n = \frac{1}{2}m(v_{n+1}^2 - v_n^2) + \frac{1}{2}\alpha(y_{n+1}^2 - y_n^2), \tag{5a}$$

$$= \frac{1}{2}m(v_{n+1} + v_n)(v_{n+1} - v_n) + \frac{1}{2}\alpha(y_{n+1} + y_n)(y_{n+1} - y_n), \tag{5b}$$

$$= \frac{1}{2}m(v_{n+1} + v_n)\frac{\Delta t}{m}\tilde{F} + \frac{1}{2}\alpha(y_{n+1} + y_n)\tilde{v}\Delta t, \tag{5c}$$

$$= -\frac{\alpha}{4}(v_{n+1} + v_n)(y_n + y_{n+1})\Delta t + \frac{\alpha}{4}(y_{n+1} + y_n)(v_{n+1} + v_n)\Delta t = 0. \tag{5d}$$

One approach to solving nonlinear problems is to take methods that have a given property for linear problems and form their convex combination. There are several ways to do this. One way involves a convex average of forces, which is

the hallmark of the Newmark family of methods,[12] and another averages positions, as is used in what is called the variational method.[13] For example, in Eq. (4), both the trapezoidal choice $\tilde{F} = (F_{n+1} + F_n)/2$ and the implicit midpoint choice $\tilde{F} = F(\bar{y})$ with $\bar{y} = (y_{n+1} + y_n)/2$ yield a conservative method for the linear problem. Their convex combination yields

$$\tilde{F} = a\frac{1}{2}(F_{n+1} + F_n) + (1-a)F(\bar{y}), \tag{6}$$

where a is a parameter. Unfortunately, this combination is not conservative for most nonlinear problems. However, this approach can be used to derive symplectic methods.[13]

III. SINGLE PARTICLE

The assumption is that a conservative numerical method for a nonlinear problem can be found by modifying a method that is known to be conservative for the linear case. For the trapezoidal method, the question is whether it is possible to find a conservative producing transitional force $\tilde{F}$ in Eq. (4). In particular, the starting assumption is that a conservative method can be found of the form

$$y_{n+1} = y_n + \frac{1}{2}[v_{n+1} + v_n]\Delta t, \tag{7}$$

$$v_{n+1} = v_n + \tilde{F}(y_{n+1}, y_n)\frac{\Delta t}{m}. \tag{8}$$

The Hamiltonian for the single particle problem, Eqs. (1) and (2), is

$$H(y,v) = \frac{1}{2}mv^2 - \int_0^y F(s)ds. \tag{9}$$

To determine $\tilde{F}$, note that

$$H_{n+1} - H_n = \frac{1}{2}m(v_{n+1}^2 - v_n^2) - \int_{y_n}^{y_{n+1}} F(s)ds, \tag{10}$$

$$= \frac{1}{2}(v_{n+1} + v_n)\left[\tilde{F}(y_{n+1}, y_n) - \frac{1}{y_{n+1} - y_n}\int_{y_n}^{y_{n+1}} F(s)ds\right]\Delta t. \tag{11}$$

It follows that the method is conservative if

$$\tilde{F}(y_{n+1}, y_n) = \frac{1}{y_{n+1} - y_n}\int_{y_n}^{y_{n+1}} F(s)ds. \tag{12}$$

The value at $y_n = y_{n+1}$ is defined using continuity, and hence $\tilde{F}(y_n, y_n) = F(y_n)$. This result shows that $\tilde{F}(y_{n+1}, y_n)$ is the average force in moving from y_n to y_{n+1}. Moreover, because $\tilde{F}(y_n, y_{n+1}) = \tilde{F}(y_{n+1}, y_n)$, $\tilde{F}(y_{n+1}, y_n)$ is the negative of the average force in moving backward from y_{n+1} to y_n. As a result, the method has time reversal symmetry. Time reversal is a property of conservative systems, and numerical experiments suggest that this property is important for preserving the qualitative long-time behavior of the numerical solution.[6]

The function $\tilde{F}$ in Eq. (12) often appears when deriving conservative numerical methods and has different names depending on the application. For example, in numerical fluid dynamics, it is related to the mean-value Jacobian.[14,15] In computational dynamics, it appears in the expression for what is called a discrete gradient.[2,4] The reason for this terminology is explained in Sec. IV.

With the derivation of Eq. (12), the resulting numerical method,

$$y_{n+1} = y_n + \frac{1}{2}(v_{n+1} + v_n)\Delta t, \tag{13}$$

$$v_{n+1} = v_n + \frac{\Delta t}{m}\frac{1}{(y_{n+1} - y_n)}\int_{y_n}^{y_{n+1}} F(s)ds, \tag{14}$$

is second order and conservative. The fact that it is conservative comes from the derivation. The proof that it is second order involves substituting the exact solution into Eqs. (13) and (14), and then expanding $y(t+\Delta t)$ and $v(t+\Delta t)$ using Taylor's theorem for small Δt. To be second order, it is required that $\tilde{F}(y_n, y_n) = F(y_n)$, and

$$\left.\frac{\partial \tilde{F}(y_{n+1}, y_n)}{\partial y_{n+1}}\right|_{y_{n+1}=y_n} = \frac{1}{2}\left.\frac{dF(y)}{dy}\right|_{y=y_n}. \tag{15}$$

It is easy to show that Eq. (12) satisfies both of these conditions, and therefore the method is second order.

The usefulness of the result in Eq. (12) for obtaining a conservative method depends on whether the integral can be done analytically or evaluated exactly. A few examples often studied in introductory courses are given in the following.

A. Examples

Power law. For the choice $F(y) = \alpha y^p$, where p is a positive integer, Eq. (12) becomes

$$\tilde{F}(y_{n+1}, y_n) = \frac{1}{y_{n+1} - y_n}\int_{y_n}^{y_{n+1}} \alpha s^p ds, \tag{16a}$$

$$= \frac{\alpha}{p+1}\frac{1}{y_{n+1} - y_n}(y_{n+1}^{p+1} - y_n^{p+1}), \tag{16b}$$

$$= \frac{\alpha}{p+1}\sum_{i=0}^{p} y_{n+1}^i y_n^{p-i}. \tag{16c}$$

In particular, for $p = 1$, Eq. (16c) for $\tilde{F}$ reduces to the expression used for the trapezoidal method.

Duffing's equation. For $\ddot{y} = -\alpha y - \beta y^3$, Eqs. (13) and (14) reduce to

$$y_{n+1} = y_n + \frac{1}{2}(v_{n+1} + v_n)\Delta t, \tag{17a}$$

$$v_{n+1} = v_n - (y_n + y_{n+1})\left[\frac{\alpha}{2} + \frac{\beta}{4}(y_n^2 + y_{n+1}^2)\right]\Delta t. \tag{17b}$$

Note that this method, which is known as Simpson's method, can be obtained from Eq. (6) by taking $a = 1/3$.[16] However, Eq. (6) is not conservative if $F(y)$ is a fourth-order polynomial, for any value of a.

Pendulum. For the pendulum, $F(y) = -\sin y$, and Eq. (12) becomes

$$\tilde{F}(y_{n+1}, y_n) = \frac{\cos(y_{n+1}) - \cos(y_n)}{y_{n+1} - y_n} = -\frac{1}{w}\sin(y_n + w)\sin w, \tag{18}$$

where $w = (v_{n+1} + v_n)\Delta t/4$.

B. Stability

To obtain a convergent numerical method, it is required that the method satisfies a stability requirement. The usual approach is to determine how the method does on linear problems. Because Eqs. (13) and (14) reduce to the trapezoidal rule for linear problems, the method qualifies as being A-stable. A-stability effectively means that if there is an asymptotically stable steady state for the linear problem, then it is also an asymptotically stable steady state for the numerical method.[17] This form of stability is mostly relevant when studying problems with stable equilibrium points.

We are interested in nonlinear oscillatory motion, which raises the question of what form of stability to consider. One possibility is to use the fact that the solution of Eqs. (13) and (14) is on the energy curve determined by the initial conditions. What this means is that the values satisfy $H(y_{n+1}, v_{n+1}) = H(y_0, v_0)$. The exact solution is also located on this curve. If the curve is compact, then the distance between the exact and numerical solution remains bounded (which is a requirement for stability).

The complication is how fast the numerical solution transverses this curve compared to the exact solution, which gives rise to the idea of phase error. As an example, if the orbit of the Earth is computed, then Eqs. (13) and (14) will find the correct orbital path. But what is not obvious is how accurately the method determines the speed at which the Earth moves along this path. In many applications, the numerical solutions of these oscillators are run over very long time intervals, and the concern is how the phase error grows in such cases. For the Earth orbit example, if the computed solution misses the terrestrial year by one day, then the error in the angular position (the phase error) is compounded if the computation is continued and used to determine the orbital location over multiple years. How to estimate the phase error analytically has been the subject of several studies.[18–20] The approach used here is to demonstrate convergence numerically.

C. Numerical experiments

The algorithm in Eqs. (13) and (14) is designed to conserve energy. One of the complications is that the method is implicit and requires finding the value of v_{n+1} that satisfies

$$v_{n+1} = v_n + \tilde{F}\left(y_n + \frac{1}{2}(v_{n+1} + v_n)\Delta t, y_n\right)\Delta t. \tag{19}$$

Accordingly, there are questions related to accuracy, both in how the solution of Eq. (19) affects energy conservation as well as the error in position and phase. There are also questions related to how Eqs. (13) and (14) compare to symplectic methods and other commonly used methods to solve initial value problems.

These questions will be addressed for the pendulum problem $\ddot{y} = -\sin y$, with $y(0) = 7\pi/8$, and $v(0) = 0$. Conservation of energy ($H = (1/2)v^2 - \cos y$) means that the solution periodically encircles the origin in the phase plane, following the energy curve:

$$\frac{1}{2}v^2 = \cos y - \cos 7\pi/8 = \cos y + \frac{1}{2}\sqrt{2 + \sqrt{2}}. \tag{20}$$

The period of the oscillation is $T = 4K(\sin(y(0)/2)^2) \approx 12.16$, where K is the elliptic integral of the first kind.

The energy conserving method in Eqs. (13) and (14) for the pendulum takes the form

$$y_{n+1} = y_n + \frac{1}{2}(v_{n+1} + v_n)\Delta t, \tag{21a}$$

$$v_{n+1} = v_n + \frac{\cos(y_{n+1}) - \cos(y_n)}{y_{n+1} - y_n}\Delta t. \tag{21b}$$

We compare Eq. (21) to the velocity-Verlet method, which is

$$y_{n+1} = y_n + v_n\Delta t - \frac{1}{2}\Delta t^2 \sin y_n, \tag{22a}$$

$$v_{n+1} = v_n - \frac{1}{2}(\sin y_{n+1} + \sin y_n)\Delta t. \tag{22b}$$

The velocity-Verlet method is a second-order symplectic method, which is conditionally convergent.[21] Another numerical solution we will consider is obtained using MATLAB's ode45 command (using the default settings and version 2017b). These choices were made for the following reasons. Symplectic methods are used extensively for molecular simulations,[22] solar system dynamics,[23] and numerous other applications where Hamiltonian systems arise.[6,8] The velocity-Verlet algorithm is well known, and is often used in these applications. The ode45 algorithm is a general purpose solver, which makes it one of the most used initial value problem solvers. It is based on an explicit Runge-Kutta method, which involves the Dormand-Prince pair of orders 4 and 5,[24] which is not symplectic and does not satisfy time reversal symmetry.

The relative differences of the computed and exact values for the energy are shown in Fig. 1. The curves shown are the computed values of $|H(t)/H(0) - 1|$, where $H(t) = H(y(t), v(t))$. The time interval corresponds to 10^3 periods of the exact solution. For Eqs. (21) and (22), 14,000 equally spaced time points were used, which corresponds to approximately 14 time steps per period. The ode45 routine is adaptive, and uses 53,753 points. Newton's root finding method was used to solve Eq. (19), with the stopping condition being an absolute error less than 10^{-14}. Note that 14,000 points were used because the velocity-Verlet algorithm is only conditionally convergent and is inaccurate with fewer points.

The maximum value of the relative energy error over the interval $0 \le t \le 1000T$ for different values of Δt is shown in Fig. 2. We see from Figs. 1 and 2 that the energy for the conservative method is significantly better than what is found using velocity-Verlet or ode45.

In addition to the requirement that the computed solution be on the curve in Eq. (20), there is also the question of where the computed solution is on this curve relative to the exact solution (that is, the phase error). One way to measure this is to compare the exact and computed number of periods over a given amount of time. So, the solution was computed for $0 \le t \le 100T$, where T is the period of the exact solution.

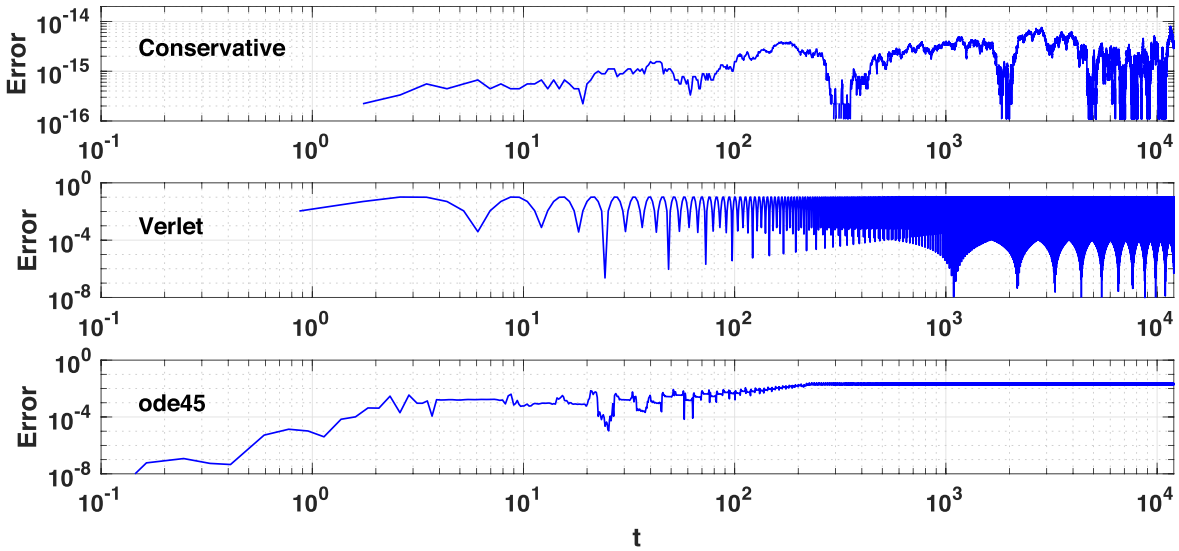

Fig. 1. The relative error $|H(t)/H(0) - 1|$ of the energy of the pendulum for $0 \le t \le 1000T$, where T is the period of the exact solution.

Figure 3 shows the number of resulting periods for the numerical solution as a function of $T/\Delta t$, which is the number of points per period. The conditional convergence of the velocity-Verlet algorithm is evident, and requires at least 14 time steps per period to obtain an accurate value for the period. In comparison, Eq. (21) yields a reasonable value for the period over the entire interval.

IV. MULTIPLE PARTICLES

The key step in the derivation of a conservative numerical method is the factorization of the difference in the Hamiltonians. To demonstrate how this can be done for a system of particles (or a single particle in more than one dimension), assume that the equation of motion is $\ddot{\mathbf{y}} = \mathbf{F}(\mathbf{y})$. We have $\dot{\mathbf{y}} = \mathbf{v}$ and

$$\dot{\mathbf{y}} = \mathbf{v}, \tag{23a}$$

$$\dot{\mathbf{v}} = \mathbf{F}(\mathbf{y}), \tag{23b}$$

where $\mathbf{F} = -\nabla V$. The Hamiltonian is $H(\mathbf{y}, \mathbf{v}) = \mathbf{v} \cdot \mathbf{v}/2 + V(\mathbf{y})$.

As before, we assume that the numerical method has the form

$$\mathbf{y}_{n+1} = \mathbf{y}_n + \frac{1}{2}(\mathbf{v}_{n+1} + \mathbf{v}_n)\Delta t, \tag{24a}$$

$$\mathbf{v}_{n+1} = \mathbf{v}_n + \tilde{\mathbf{F}}(\mathbf{y}_{n+1}, \mathbf{y}_n)\Delta t. \tag{24b}$$

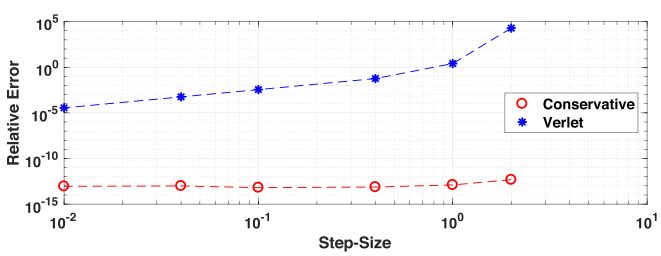

Fig. 2. Maximum relative error of the total energy as a function of the step size Δt used to solve the pendulum equation.

In this case,

$$H(\mathbf{y}_{n+1}, \mathbf{v}_{n+1}) - H(\mathbf{y}_n, \mathbf{v}_n) = \frac{1}{2}(\mathbf{v}_{n+1}^2 - \mathbf{v}_n^2) + V(\mathbf{y}_{n+1}) - V(\mathbf{y}_n), \tag{25a}$$

$$= \frac{1}{2}(\mathbf{v}_{n+1} + \mathbf{v}_n) \cdot (\mathbf{v}_{n+1} - \mathbf{v}_n) + V(\mathbf{y}_{n+1}) - V(\mathbf{y}_n), \tag{25b}$$

$$= \frac{1}{2}(\mathbf{v}_{n+1} + \mathbf{v}_n) \cdot \tilde{\mathbf{F}}\Delta t + V(\mathbf{y}_{n+1}) - V(\mathbf{y}_n). \tag{25c}$$

We assume that the potential energy difference can be factored as

$$V(\mathbf{y}_{n+1}) - V(\mathbf{y}_n) = (\mathbf{y}_{n+1} - \mathbf{y}_n) \cdot \mathbf{Q}(\mathbf{y}_{n+1}, \mathbf{y}_n). \tag{26}$$

Hence,

$$H(\mathbf{y}_{n+1}, \mathbf{v}_{n+1}) - H(\mathbf{y}_n, \mathbf{v}_n) = \frac{1}{2}(\mathbf{v}_{n+1} + \mathbf{v}_n) \cdot \tilde{\mathbf{F}}\Delta t + (\mathbf{y}_{n+1} - \mathbf{y}_n) \cdot \mathbf{Q}, \tag{27a}$$

$$= \frac{1}{2}(\mathbf{v}_{n+1} + \mathbf{v}_n) \cdot \tilde{\mathbf{F}}\Delta t + \frac{1}{2}(\mathbf{v}_{n+1} + \mathbf{v}_n) \cdot \mathbf{Q}\Delta t, \tag{27b}$$

$$= \frac{1}{2}(\mathbf{v}_{n+1} + \mathbf{v}_n) \cdot (\tilde{\mathbf{F}} + \mathbf{Q})\Delta t. \tag{27c}$$

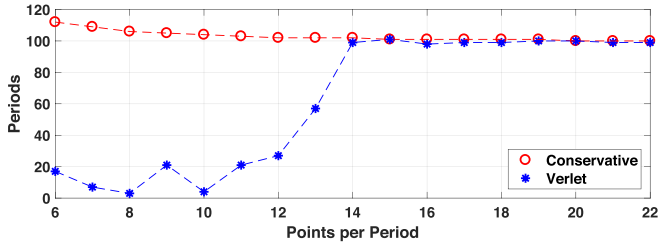

Fig. 3. Number of periods for the numerical solution of the pendulum problem for $0 \le t \le 100T$, where T is the period of the exact solution. The points per period is $T/\Delta t$.

To obtain a conservative method, we take $\tilde{\mathbf{F}} = -\mathbf{Q}$.

The factorization in Eq. (26) is the essential step in the derivation. Equation (26) is required to hold for all $\mathbf{y}_{n+1}$ and $\mathbf{y}_n$, which means that it is also true that $V(\mathbf{y}_n) - V(\mathbf{y}_{n+1}) = (\mathbf{y}_n - \mathbf{y}_{n+1}) \cdot \mathbf{Q}(\mathbf{y}_n, \mathbf{y}_{n+1})$. Together with Eq. (26), it follows that $\mathbf{Q}$ must satisfy the symmetry condition:

$$\mathbf{Q}(\mathbf{y}_{n+1}, \mathbf{y}_n) = \mathbf{Q}(\mathbf{y}_n, \mathbf{y}_{n+1}). \tag{28}$$

The value for $\mathbf{y}_{n+1} = \mathbf{y}_n$ is defined using continuity. One way to determine this value is to use Taylor's theorem for $\mathbf{y}_{n+1}$ near $\mathbf{y}_n$, which gives $V(\mathbf{y}_{n+1}) = V(\mathbf{y}_n) + (\mathbf{y}_{n+1} - \mathbf{y}_n) \cdot \nabla V(\mathbf{y}_n) + \cdots$. From this result, we conclude that

$$\mathbf{Q}(\mathbf{y}_n, \mathbf{y}_n) = \nabla V(\mathbf{y}_n). \tag{29}$$

The form of Eq. (29) explains why $\mathbf{Q}(\mathbf{y}_{n+1}, \mathbf{y}_n)$ is often referred to as a discrete gradient.[4]

Coupled linear oscillators. For $\mathbf{F} = -\mathbf{A}\mathbf{y}$, where $\mathbf{A}$ is symmetric, the potential energy function is $V(\mathbf{y}) = (1/2)\mathbf{y}^T\mathbf{A}\mathbf{y}$. In this case, from Eq. (26),

$$V(\mathbf{y}_{n+1}) - V(\mathbf{y}_n) = \frac{1}{2}\mathbf{y}_{n+1}^T\mathbf{A}\mathbf{y}_{n+1} - \frac{1}{2}\mathbf{y}_n^T\mathbf{A}\mathbf{y}_n, \tag{30a}$$

$$= \frac{1}{2}(\mathbf{y}_{n+1} - \mathbf{y}_n)^T\mathbf{A}(\mathbf{y}_{n+1} + \mathbf{y}_n). \tag{30b}$$

To obtain a conservative method, we take $\tilde{\mathbf{F}} = -\mathbf{A}(\mathbf{y}_{n+1} + \mathbf{y}_n)/2$. This result is not unexpected because the resulting numerical method is the trapezoidal method for a linear system.

Conservative central force. We take $\mathbf{F} = -\nabla V(||\mathbf{y}||)$. Then Eq. (26) requires that $V(||\mathbf{y}_{n+1}||) - V(||\mathbf{y}_n||) = (\mathbf{y}_{n+1} - \mathbf{y}_n) \cdot \mathbf{Q}(\mathbf{y}_{n+1}, \mathbf{y}_n)$. If we assume that $\mathbf{Q} = \alpha(\mathbf{y}_{n+1} + \mathbf{y}_n)$, we find

$$\tilde{\mathbf{F}} = -\frac{V(||\mathbf{y}_{n+1}||) - V(||\mathbf{y}_n||)}{||\mathbf{y}_{n+1}||^2 - ||\mathbf{y}_n||^2}(\mathbf{y}_{n+1} + \mathbf{y}_n). \tag{31}$$

Van der Waals interaction. For a one-dimensional model of interacting hydrogen atoms, the Hamiltonian is[25,26]

$$H = \frac{1}{2}m\mathbf{v} \cdot \mathbf{v} + \frac{1}{2}\omega_0^2\mathbf{y} \cdot \mathbf{y} + \frac{e^2}{4\pi}\left(\frac{1}{R} + \frac{1}{R + y_1 - y_2} - \frac{1}{R + y_1} - \frac{1}{R - y_2}\right), \tag{32}$$

where R is the atomic separation and $\mathbf{v} = \dot{\mathbf{y}}$. In this case, letting $\mathbf{y}_{n+1} = (y_{1,n+1}, y_{2,n+1})$ and $\mathbf{y}_n = (y_{1,n}, y_{2,n})$,

$$V(\mathbf{y}_{n+1}) - V(\mathbf{y}_n) = \frac{1}{2}\omega_0^2(\mathbf{y}_{n+1} \cdot \mathbf{y}_{n+1} - \mathbf{y}_n \cdot \mathbf{y}_n) + \frac{e^2}{4\pi}\left(\frac{1}{R + y_{1,n+1} - y_{2,n+1}} - \frac{1}{R + y_{1,n+1}} - \frac{1}{R - y_{2,n+1}}\right) - \frac{e^2}{4\pi}\left(\frac{1}{R + y_{1,n} - y_{2,n}} - \frac{1}{R + y_{1,n}} - \frac{1}{R - y_{2,n}}\right), \tag{33a}$$

$$= \frac{1}{2}\omega_0^2(\mathbf{y}_{n+1} - \mathbf{y}_n) \cdot (\mathbf{y}_{n+1} + \mathbf{y}_n) + \frac{e^2}{4\pi}\frac{y_{1,n} - y_{1,n+1} + y_{2,n+1} - y_{2,n}}{(R + y_{1,n+1} - y_{2,n+1})(R + y_{1,n} - y_{2,n})} + \frac{e^2}{4\pi}\left(\frac{y_{1,n+1} - y_{1,n}}{(R + y_{1,n+1})(R + y_{1,n})} + \frac{y_{2,n} - y_{2,n+1}}{(R - y_{2,n+1})(R - y_{2,n})}\right). \tag{33b}$$

From Eq. (33b), it follows that $\tilde{\mathbf{F}} = -\omega_0^2(\mathbf{y}_{n+1} + \mathbf{y}_n)/2 - e^2\mathbf{P}/4\pi$, where $\mathbf{P} = (P_1, P_2)$, with

$$P_1 = \frac{-1}{(R + y_{1,n+1} - y_{2,n+1})(R + y_{1,n} - y_{2,n})} + \frac{1}{(R + y_{1,n+1})(R + y_{1,n})}, \tag{34a}$$

and

$$P_2 = \frac{1}{(R + y_{1,n+1} - y_{2,n+1})(R + y_{1,n} - y_{2,n})} + \frac{-1}{(R - y_{2,n+1})(R - y_{2,n})}. \tag{34b}$$

Hénon-Heiles model. The Hénon-Heiles model for the planar motion of a star in a galaxy can be expressed as[27]

$$\dot{x} = u, \tag{35a}$$

$$\dot{y} = w, \tag{35b}$$

$$\dot{u} = -ax - 2xy, \tag{35c}$$

$$\dot{w} = -by - x^2 + cy^2. \tag{35d}$$

The corresponding potential energy function is $V = 1/2(ax^2 + by^2) + x^2y - (1/3)cy^3$. Let $\mathbf{y}_n = (x_n, y_n)^T$ be the current value and $\mathbf{y}_{n+1} = (x_{n+1}, y_{n+1})^T$ be the value at the next time step. To find the factorization of the difference in the potential energies as required in Eq. (26), we have

$$V(\mathbf{y}_{n+1}) - V(\mathbf{y}_n) = a(x_{n+1}^2 - x_n^2)/2 + b(y_{n+1}^2 - y_n^2)/2 - c(y_{n+1}^3 - y_n^3)/3 + x_{n+1}^2y_{n+1} - x_n^2y_n, \tag{36a}$$

$$= (\mathbf{y}_{n+1} - \mathbf{y}_n) \cdot \mathbf{R} + x_{n+1}^2y_{n+1} - x_n^2y_n, \tag{36b}$$

where $\mathbf{R} = (a(x_{n+1} + x_n)/2, b(y_{n+1} + y_n)/2 - c(y_{n+1}^2 + y_ny_{n+1} + y_n^2)/3)^T$. It remains to find P and Q so that $x_{n+1}^2y_{n+1} - x_n^2y_n = (x_{n+1} - x_n)P + (y_{n+1} - y_n)Q$. After a short calculation, we find that $Q = (x_n^2 + x_{n+1}^2)/2$ and $P = (x_ny_n + x_ny_{n+1} + x_{n+1}y_n + x_{n+1}y_{n+1})/2$. The resulting conservative method for solving the Hénon-Heiles model is

$$x_{n+1} = x_n + \frac{1}{2}\Delta t(u_{n+1} + u_n), \tag{37a}$$

$$y_{n+1} = y_n + \frac{1}{2}\Delta t(w_{n+1} + w_n), \tag{37b}$$

$$u_{n+1} = u_n - \frac{1}{2}\Delta t[a(x_{n+1}+x_n) + x_n y_n + x_n y_{n+1} + x_{n+1} y_n + x_{n+1} y_{n+1}], \tag{37c}$$

$$w_{n+1} = w_n - \frac{1}{2}\Delta t\left[b(y_{n+1}+y_n) + x_n^2 + x_{n+1}^2\right] + \frac{1}{3}ck(y_{n+1}^2 + y_n y_{n+1} + y_n^2). \tag{37d}$$

V. APPLICATION: CHAIN OF NONLINEAR OSCILLATORS

An interesting system is the motion of a chain of identical masses and springs. For nearest-neighbor interactions, the equations of motion are

$$m\ddot{y}_\alpha = \dot{V}_s(y_{\alpha+1} - y_\alpha) - \dot{V}_s(y_\alpha - y_{\alpha-1}) \quad (\alpha = 1, 2, \ldots N), \tag{38}$$

where $y_\alpha(t)$ is the displacement of particle α relative to its equilibrium location, m is its mass, and $V_s(y)$ is the interaction potential. This system is illustrated in Fig. 4, where the springs between the masses each have potential V_s.

The Hamiltonian for this system is

$$H = \frac{1}{2}m\mathbf{v}\cdot\mathbf{v} + \sum_{\alpha=1}^{N+1} V_s(y_\alpha - y_{\alpha-1}), \tag{39}$$

where $\mathbf{v} = \dot{\mathbf{y}}$ and $\mathbf{y}$ is the vector of particle displacements. It is assumed in the following that, $y_0 = y_{N+1} = 0$, and $m = 1$.

To use the conservative method we have discussed, it is necessary to find the factorization

$$\sum_{\alpha=1}^{N+1}\left[V_s(y_{\alpha,n+1} - y_{\alpha-1,n+1}) - V_s(y_{\alpha,n} - y_{\alpha-1,n})\right] = (\mathbf{y}_{n+1} - \mathbf{y}_n)\cdot\mathbf{Q}(\mathbf{y}_{n+1}, \mathbf{y}_n), \tag{40}$$

where $y_{\alpha,n}$ is the displacement of particle α at time t_n. The difficulty of finding the factorization depends on the form of V_s. In what follows, we will assume that the potential function is

$$V_s(y) = \frac{1}{2}k_1 y^2 + \frac{1}{4}k_2 y^4. \tag{41}$$

The quartic term in Eq. (41) leads to what is sometimes called the β-model for the Fermi-Pasta-Ulam (FPU) problem, which has been used to study crystal dislocation, localized excitations in ionic crystals, and thermal denaturation of DNA.[28,29]

To find the factorization, it is convenient to write $V_s = V_1 + V_2$, where $V_1 = k_1 y^2/2$ and $V_2 = k_2 y^4/4$.

Note that

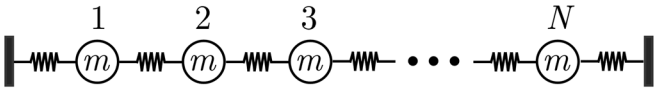

Fig. 4. Chain of masses and springs.

$$\sum_{\alpha=1}^{N+1}\left[V_1(y_{\alpha,n+1} - y_{\alpha-1,n+1}) - V_1(y_{\alpha,n} - y_{\alpha-1,n})\right] = \frac{1}{2}k_1\sum\left[(y_{\alpha,n+1} - y_{\alpha-1,n+1})^2 - (y_{\alpha,n} - y_{\alpha-1,n})^2\right], \tag{42a}$$

$$= \frac{1}{2}k_1\sum(y_{\alpha,n+1} - y_{\alpha,n})(-y_{\alpha-1,n+1} + 2y_{\alpha,n+1} - y_{\alpha+1,n+1} - y_{\alpha-1,n} + 2y_{\alpha,n} - y_{\alpha+1,n}), \tag{42b}$$

$$= (\mathbf{y}_{n+1} - \mathbf{y}_n)\cdot\mathbf{Q}_1, \tag{42c}$$

where $\mathbf{Q}_1 = \frac{1}{2}k_1\mathbf{A}(\mathbf{y}_{n+1} + \mathbf{y}_n)$ and $\mathbf{A}$ is the $N\times N$ tridiagonal matrix with 2's on the diagonal, and –1's on the super- and sub-diagonals. Also,

$$\sum_{\alpha=1}^{N+1}\left[V_2(y_{\alpha,n+1} - y_{\alpha-1,n+1}) - V_2(y_{\alpha,n} - y_{\alpha-1,n})\right] = \frac{1}{4}k_2\sum\left[(y_{\alpha,n+1} - y_{\alpha-1,n+1})^4 - (y_{\alpha,n} - y_{\alpha-1,n})^4\right], \tag{43a}$$

$$= \frac{1}{4}k_2\sum(y_{\alpha,n+1} - y_{\alpha,n})\left[(y_{\alpha,n+1} + y_{\alpha,n})B_\alpha + C_\alpha\right], \tag{43b}$$

$$= (\mathbf{y}_{n+1} - \mathbf{y}_n)\cdot\mathbf{Q}_2, \tag{43c}$$

where

$$B_\alpha = 2(y_{\alpha,n+1}^2 + y_{\alpha,n}^2) + 3(y_{\alpha-1,n+1}^2 + y_{\alpha-1,n}^2 + y_{\alpha+1,n+1}^2 + y_{\alpha+1,n}^2), \tag{44}$$

$$C_\alpha = -2\Big[y_{\alpha-1n+1}^3 + y_{\alpha-1,n}^3 + y_{\alpha+1,n+1}^3 + y_{\alpha+1,n}^3 + (y_{\alpha-1,n+1} + y_{\alpha-1,n} + y_{\alpha+1n+1} + y_{\alpha+1,n})\times\left(y_{\alpha,n+1}^2 + y_{\alpha,n+1}y_{\alpha,n} + y_{\alpha,n}^2\right)\Big], \tag{45}$$

and

$$(\mathbf{Q}_2)_\alpha = \frac{1}{4}k_2\left[(y_{\alpha,n+1} + y_{\alpha,n})B_\alpha + C_\alpha\right]. \tag{46}$$

The resulting conservative method is given in Eq. (24), where

$$\tilde{\mathbf{F}}(\mathbf{y}_{n+1}, \mathbf{y}_n) = -\frac{1}{2}k_1\mathbf{A}(\mathbf{y}_{n+1} + \mathbf{y}_n) - \mathbf{Q}_2(\mathbf{y}_{n+1}, \mathbf{y}_n). \tag{47}$$

The implementation of the conservative method, using the force in Eq. (47), requires finding $\mathbf{v}_{n+1}$ by solving

$$\mathbf{v}_{n+1} = \mathbf{v}_n + \tilde{\mathbf{F}}\left(\mathbf{y}_n + \frac{1}{2}(\mathbf{v}_{n+1} + \mathbf{v}_n)\Delta t, \mathbf{y}_n\right)\Delta t. \tag{48}$$

In what follows, Eq. (48) is solved using Newton's method. Note that because of the assumption of nearest-neighbor interactions, the Jacobian needed for Newton's method is tridiagonal, which reduces the computational cost of solving for $\mathbf{v}_{n+1}$.

To explain some of the choices for computing the solution of the nonlinear problem, we recall some properties of the linear problem. Specifically, for $k_2 = 0$, the natural frequencies of the problem are

$$\omega_j = 2\sqrt{\frac{k_1}{m}}\sin(j\theta/2) \quad (j = 1, 2, \ldots, N), \tag{49}$$

where $\theta = \pi/(N+1)$. The associated natural modes are

$$\mathbf{x}_j = \sqrt{\frac{2}{N+1}}(\sin(j\theta), \sin(2j\theta), \sin(3j\theta), \ldots, \sin(Nj\theta))^T. \tag{50}$$

Note that the $\mathbf{x}_j$'s are an orthonormal basis for $\mathbb{R}^N$.

The initial condition to be used for the nonlinear problem comes from the third natural mode, and so $y_\alpha(0) = \sin(3\alpha\theta)$ and $v_\alpha(0) = 0$. We will take $N = 32$, $m = 1$, $k_1 = 1$, and $k_2 = 5$. To determine the time step, note that the periods of the linear modes vary from $2\pi/\omega_1 \approx 2(N+1)$ down to $2\pi/\omega_N \approx \pi$. To guarantee that there are at least three time steps per linear period, we take $\Delta t \leq 1$. We use for the stopping condition for Newton's method that the error is less than 10^{-14}.

The solution is computed for $0 < t \leq 10{,}000$ and the maximum relative energy error is determined over this interval. This error is defined as $\max|H(t)/H(0) - 1|$. The value of this error as a function of the value of Δt is shown in Fig. 5. Also shown are the values obtained using the velocity-Verlet algorithm. Note that the latter method is only conditionally stable, and requires a time step no larger than about 0.4.

The results in Fig. 5 are not surprising and show that Eq. (24) produces a solution with an energy close to machine precision. The velocity-Verlet algorithm gives an inaccurate energy value for large step sizes but improves quickly as the step size is decreased. For each value of Δt, velocity-Verlet is significantly faster than Eq. (24). As an example, when $\Delta t = 0.25$, velocity-Verlet is about 100 times faster. However, for velocity-Verlet to achieve the same error that the conservative method has when $\Delta t = 1$, it is necessary to take a very small step size. Although the value of Δt can be estimated from Fig. 5, we stress that there is a significant increase in computing time to achieve an equivalent error. In particular, even for $\Delta t = 0.001$, velocity-Verlet takes approximately 15 times longer than Eq. (24) using $\Delta t = 1$ yet the energy error is several orders of magnitude larger.

Measuring the phase error in this problem is more challenging than for the single degree of freedom pendulum. One possible approach is to use the orthonormal basis coming from the linear problem. In particular, it is possible to write

$$\mathbf{y}(t) = c_1(t)\mathbf{x}_1 + c_2(t)\mathbf{x}_2 + \cdots + c_N(t)\mathbf{x}_N, \tag{51}$$

where the $\mathbf{x}_j$'s are given in Eq. (50) and

$$c_j(t) = \mathbf{y}\cdot\mathbf{x}_j = \sqrt{\frac{2}{N+1}}\sum_{\alpha=1}^{N} y_\alpha(t)\sin(\alpha j\theta). \tag{52}$$

The un-normalized first mode will be used for the initial condition, so $y_\alpha(0) = \sin(\alpha\theta)$, and $v_\alpha(0) = 0$. The solution $\mathbf{y}(t)$ is computed for $0 \leq t \leq 12{,}000$, and then the basis coefficients $c_j(t)$ are found using Eq. (52). The resulting values for $c_1(t)$, $c_3(t)$, and $c_5(t)$ are plotted in Fig. 6. It is seen that each c_j oscillates rapidly, corresponding to the frequency ω_j in Eq. (49). We will concentrate on $c_1(t)$, because it is associated with the initial condition. There is a slow periodic modulation of $c_1(t)$, with a period of about 6500. In the early analyses of the FPU problem, this period generated much excitement and was termed a superperiod.[30] This is often seen in nonlinear oscillator motion, and it is possible to derive expressions for the modulated period in certain cases using the method of multiple scales.[31]

For the value of Δt used in Fig. 6, both Eq. (24) and the velocity-Verlet algorithm determine the period of the fast oscillation of $c_1(t)$ very well. The challenge lies in computing the value of the superperiod. The superperiod is determined here by computing the time between the local minima in the envelope of $c_1(t)$ as shown in Fig. 6. The resulting values of the relative error in the period are given in Fig. 7 as a function of Δt, obtained using Eq. (24) and velocity-Verlet. It is seen that the two methods have similar accuracy.

VI. SUMMARY

The factorization in Eq. (26) has a long history, going back to at least the work of LaBudde and Greenspan[3,32] who used it to derive Eq. (31). The general version was derived a short time later.[33] It is easy to generalize the method so that it works for more general Hamiltonian systems,[4,6,34] systems with multiple invariants,[6,34,35] and conservative partial differential equations.[36,37]

The resulting numerical method is capable of producing a conservative solution to machine precision, and is A-stable. Its usefulness depends on finding the discrete gradient. Several examples were given, but in many real world problems, it can be difficult to find $\mathbf{Q}$. The other serious criticism of the method is that it is implicit, which means longer computing times for a given time step compared to explicit symplectic methods. To quantify this point, computing an

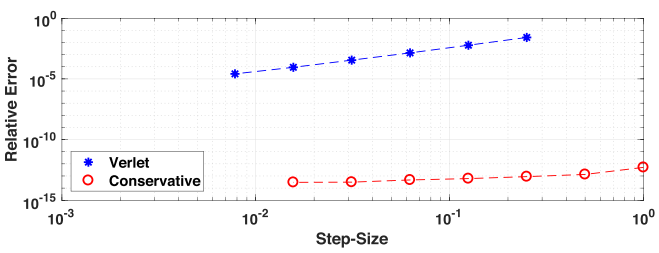

Fig. 5. Relative energy error as a function of the time step used to solve the FPU problem for $0 \leq t \leq 10,000$.

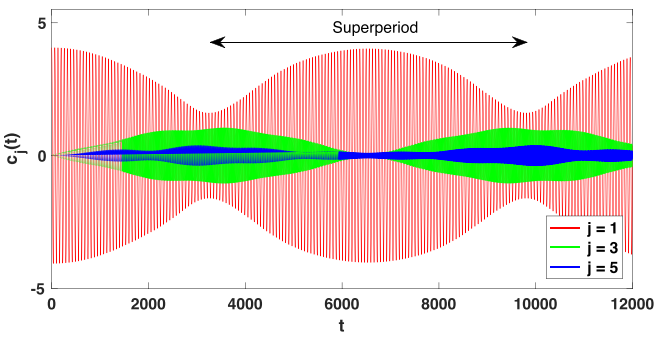

Fig. 6. The coefficients $c_1(t)$, $c_3(t)$, and $c_5(t)$ in Eq. (51) for the coupled oscillators with $y_\alpha(0) = \sin(\alpha\theta)$, and $v_\alpha(0) = 0$. In this calculation, $\Delta t = 0.1$.

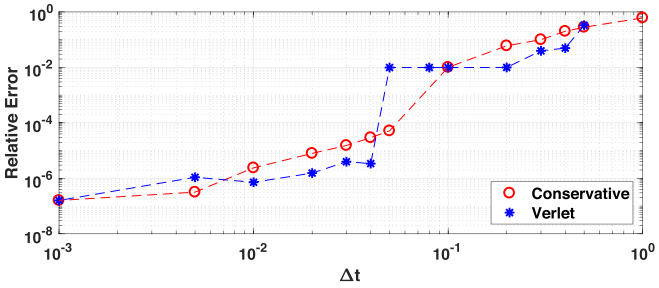

Fig. 7. Relative error of the computed value for the superperiod illustrated in Fig. 6 as a function of the step size used to solve the FPU problem.

accurate value for $\mathbf{v}_{n+1}$ requires about four iteration steps in Newton's method. For the simple examples considered here, the increase in computing time is minimal. For more physically realistic problems, evaluating the forcing term can be very time consuming. In these cases, the implicit conservative method can take significantly longer than explicit symplectic methods. It is possible that the time required for a force evaluation can be appreciably reduced on a GPU, or a multicore CPU, but whether this can be done effectively is an open question.

To conclude, numerical methods have been derived that satisfy conservation of energy to machine precision, albeit with more computing time compared to explicit symplectic methods. It is appropriate to end with a comment by Seymour Cray. CRAY supercomputers at the time held the computing speed record, but questions arose about the inaccuracy of certain calculations on these machines. It turned out that arithmetic error checks were not being made, which helped speed up the computations. When asked about this, his reply was "do you want it fast or do you want it correct?"[38]

VII. SUGGESTED PROBLEMS

Problem 1. Suppose a mass is situated between two parallel walls and is connected to the walls by springs as shown in Fig. 8. The restoring force in this case has the form

$$F(y) = -y\left[1 - \frac{\lambda}{\sqrt{1+y^2}}\right], \tag{53}$$

where $0 < \lambda < 1$.

(a) Show that Eq. (14) reduces to

$$v_{n+1} = v_n - (y_{n+1} + y_n) \times \left[\frac{1}{2} - \lambda \frac{1}{\sqrt{1+y_{n+1}^2} + \sqrt{1+y_n^2}}\right]\frac{\Delta t}{m}. \tag{54}$$

(b) For $\lambda = 0.5$, $y(0) = 1$, and $v(0) = 0$, the period is $T \approx 8$. Compute the solution using the conservative method for $0 \le t \le 1000T$, using 20 time steps per period. Then plot the resulting relative Hamiltonian error $|H(t)/H(0) - 1|$, similar to what was done in Fig. 1.

(c) The velocity-Verlet method for solving Eqs. (13) and (14) is

$$y_{n+1} = y_n + v_n\Delta t + F_n\frac{\Delta t^2}{2m}, \tag{55a}$$

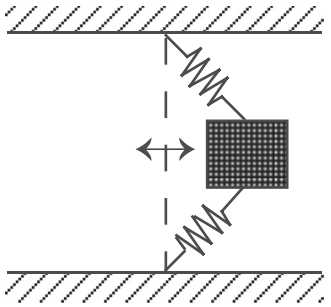

Fig. 8. Oscillator studied in Problem 1.

$$v_{n+1} = v_n + (F_{n+1} + F_n)\frac{\Delta t}{2m}. \tag{55b}$$

Redo part (b) using the velocity-Verlet method.

(d) How do the errors in parts (b) and (c) compare? If the number of time steps per period is doubled or cut in half, how do the methods compare?

Problem 2. Let $V(y)$ be the associated potential for the single particle problem in Eqs. (1) and (2), so that $F(y) = -V'(y)$.

(a) Show that Eq. (14) can be written as

$$v_{n+1} = v_n - \frac{V(y_{n+1}) - V(y_n)}{y_{n+1} - y_n}\frac{\Delta t}{m}. \tag{56}$$

(b) The Toda potential is $V(y) = e^y - y$. What is the corresponding force $F(y)$? Show that the result in part (a) reduces to

$$v_{n+1} = v_n + \left(1 - \frac{e^{y_{n+1}} - e^{y_n}}{y_{n+1} - y_n}\right)\frac{\Delta t}{m}. \tag{57}$$

(c) Finding v_{n+1} from Eq. (56) requires solving $f(v_{n+1}) = 0$, where

$$f(x) \equiv x - v_n + \frac{V(y_{n+1}) - V(y_n)}{y_{n+1} - y_n}\frac{\Delta t}{m}, \tag{58}$$

and $y_{n+1} = y_n + (1/2)(x + v_n)\Delta t$. If Newton's method is used to solve this equation, it is necessary to find $f'(x)$. Show that

$$f'(x) = 1 - \frac{V(y_{n+1}) - V(y_n) + (y_{n+1} - y_n)F(y_{n+1})}{(y_{n+1} - y_n)^2}\frac{\Delta t^2}{2m}. \tag{59}$$

(d) If $y(0) = 1$, and $v(0) = 0$ for the Toda potential in part (b), the period is $T \approx 6.7$. Use the result from part (c) and find $y(t)$ and $v(t)$ using the conservative method for $0 \le t \le 1000T$ with 10 time steps per period. Plot the resulting relative error $|H(t)/H(0) - 1|$, as was done in Fig. 1. The stopping condition for Newton's method should be an absolute error less that 10^{-12}.

(e) Redo part (d) using the velocity-Verlet method. The general form for velocity-Verlet is given in Problem 1(c).

(f) How do the errors in parts (d) and (e) compare? If the number of time steps per period is doubled, or cut in half, how do the methods compare?

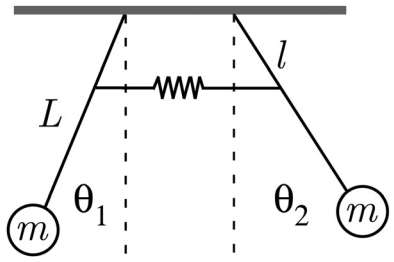

Fig. 9. Coupled pendulums studied in Exercise 3.

Problem 3. Two pendulums are coupled by a spring, as shown in Fig. 9. The pendulums have the same mass m and length L. Let k be the spring constant, and assume that the spring is attached a distance ℓ from the upper pivot (as measured along the rod of each pendulum). The resulting equations of motion are

$$mL^2\ddot{\theta}_1 = -mgL\sin\theta_1 + k\ell^2 f(\sin\theta_2, \sin\theta_1)\cos\theta_1, \tag{60a}$$

$$mL^2\ddot{\theta}_2 = -mgL\sin\theta_2 - k\ell^2 f(\sin\theta_2, \sin\theta_1)\cos\theta_2, \tag{60b}$$

where $f(\sin\theta_2, \sin\theta_1) = \sin\theta_2 - \sin\theta_1$. In this problem, $\mathbf{y} = (\theta_1, \theta_2)^T$ and $\mathbf{v} = (\dot{\theta}_1, \dot{\theta}_2)^T$. Show that $\mathbf{Q} = (Q_1, Q_2)$, where

$$Q_1 = \frac{1}{\theta_{1,n+1} - \theta_{1,n}}\left[-\alpha(\cos\theta_{1,n+1} - \cos\theta_{1,n}) + \frac{\beta}{2} f(\theta_{1,n+1}, \theta_{1,n})\left(f(\theta_{1,n+1}, \theta_{2,n+1}) + f(\theta_{1,n}, \theta_{2,n})\right)\right], \tag{61a}$$

and

$$Q_2 = \frac{1}{\theta_{2,n+1} - \theta_{2,n}}\left[-\alpha(\cos\theta_{2,n+1} - \cos\theta_{2,n}) + \frac{\beta}{2} f(\theta_{2,n+1}, \theta_{2,n})\left(f(\theta_{2,n+1}, \theta_{1,n+1}) + f(\theta_{2,n}, \theta_{1,n})\right)\right], \tag{61b}$$

where $\alpha = g/L$, $\beta = k\ell^2/(mL^2)$, and $\theta_{1,n}$ is the value of θ_1 at time t_n, with similar meanings for the other angular variables.

ACKNOWLEDGMENT

This work was supported, in part, by the NSF through Grant No. DMS-1122279.

[1]J. M. Sanz-Serna, "Runge-Kutta schemes for Hamiltonian systems," BIT **28**(4), 877–883 (1988).
[2]O. Gonzalez, "Time integration and discrete Hamiltonian systems," J. Nonlinear Sci. **6**(5), 449–467 (1996).
[3]R. A. LaBudde and D. Greenspan, "Energy and momentum conserving methods of arbitrary order for the numerical integration of equations of motion. I. Motion of a single particle," Numer. Math. **25**(4), 323–346 (1975).
[4]R. I. McLachlan, G. R. W. Quispel, and N. Robidoux, "Geometric integration using discrete gradients," Philos. Trans. R. Soc. London A **357**(1754), 1021–1045 (1999).
[5]R. I. McLachlan and G. R. W. Quispel, "Geometric integrators for ODEs," J. Phys. A: Math. Gen. **39**(19), 5251–5285 (2006).
[6]E. Hairer, C. Lubich, and G. Wanner, *Geometric Numerical Integration: Structure-Preserving Algorithms for Ordinary Differential Equations*, 2nd ed. (Springer, New York, 2010).
[7]D. Donnelly and E. Rogers, "Symplectic integrators: An introduction," Am. J. Phys. **73**(10), 938–945 (2005).
[8]B. Leimkuhler and S. Reich, *Simulating Hamiltonian Dynamics* (Cambridge U.P., Cambridge, 2004).
[9]A. Lew, J. E. Marsden, M. Ortiz, and M. West, "An overview of variational integrators," in *Finite Element Methods: 1970's and Beyond*, edited by L. P. Franca, T. E. Tezduyar, and A. Masud (CIMNE, Barcelona, Spain, 2004), pp. 98–115.
[10]G. Zhong and J. E. Marsden, "Lie-Poisson Hamilton-Jacobi theory and Lie-Poisson integrators," Phys. Lett. A **133**(3), 134–139 (1988).
[11]C. Kane, J. E. Marsden, and M. Ortiz, "Symplectic-energy-momentum preserving variational integrators," J. Math. Phys. **40**(7), 3353–3371 (1999).
[12]M. Geradin and D. Rixen, *Mechanical Vibrations: Theory and Applications to Structural Dynamics*, 2nd ed. (John Wiley & Sons, Chichester, England, 1997).
[13]C. Kane, J. E. Marsden, M. Ortiz, and M. West, "Variational integrators and the Newmark algorithm for conservative and dissipative mechanical systems," Int. J. Numer. Methods Eng. **49**(10), 1295–1325 (2000).
[14]A. Harten, "On high resolution schemes for hyperbolic conservation laws," J. Comput. Phys. **49**(3), 357–393 (1983).
[15]P. L. Roe, "Approximate Riemann solvers, parameter vectors, and difference schemes," J. Comput. Phys. **43**(3), 357–372 (1981).
[16]E. Celledoni, R. I. McLachlan, B. Owren, and G. R. W. Quispel, "Geometric properties of Kahan's method," J. Phys. A: Math. Gen. **46**(2), 025201 (2013).
[17]M. H. Holmes, *Introduction to Scientific Computing and Data Analysis* (Springer, New York, 2016).
[18]R. I. McLachlan, M. Perlmutter, and G. R. W. Quispel, "On the nonlinear stability of symplectic integrators," BIT Numer. Math. **44**(1), 99–117 (2004).
[19]B. Cano and J. M. Sanz-Serna, "Error growth in the numerical integration of periodic orbits, with application to Hamiltonian and reversible systems," SIAM J. Numer. Anal. **34**(4), 1391–1417 (1997).
[20]M. Calvo, M. P. Laburta, J. I. Montijano, and L. Randez, "Error growth in the numerical integration of periodic orbits," Math. Comput. Simul. **81**(12), 2646–2661 (2011).
[21]M. H. Holmes, *Introduction to Numerical Methods in Differential Equations* (Springer, New York, 2007).
[22]T. Schlick, *Molecular Modeling and Simulation: An Interdisciplinary Guide*, 2nd ed. (Springer, New York, 2010).
[23]A. Morbidelli, "Modern integrations of solar system dynamics," Ann. Rev. Earth Planet. Sci. **30**(1), 89–112 (2002).
[24]L. Shampine, *Numerical Solution of Ordinary Differential Equations* (Chapman and Hall/CRC, London, 1994).
[25]B. R. Holstein, "The van der Waals interaction," Am. J. Phys. **69**(4), 441–449 (2001).
[26]C. Kittel, *Introduction to Solid State Physics*, 8th ed. (John Wiley & Sons, Hoboken, NJ, 2005).
[27]M. Hénon and C. Heiles, "The applicability of the third integral of motion: Some numerical experiments," Astron. J. **69**, 73–79 (1964).
[28]G. Gallavotti, *The Fermi-Pasta-Ulam Problem: A Status Report* (Springer, New York, 2008).
[29]T. P. Weissert, *The Genesis of Simulation in Dynamics: Pursuing the Fermi-Pasta-Ulam Problem* (Springer, New York, 2012).
[30]J. L. Tuck and M. T. Menzel, "The superperiod of the nonlinear weighted string (FPU) problem," Adv. Math. **9**(3), 399–407 (1972).
[31]M. H. Holmes, *Introduction to Perturbation Methods*, 2nd ed. (Springer-Verlag, New York, 2013).
[32]R. A. LaBudde and D.Greenspan, "Energy and momentum conserving methods of arbitrary order for the numerical integration of equations of motion. II. Motion of a system of particles," Numer. Math. **26**(1), 1–16 (1976).

[33]A. J. Chorin, T. J. R. Hughes, M. F. McCracken, and J. E. Marsden, "Product formulas and numerical algorithms," Commun. Pure Appl. Math. **31**(2), 205–256 (1978).
[34]J. C. Simo, N. Tarnow, and K. K. Wong, "Exact energy-momentum conserving algorithms and symplectic schemes for nonlinear dynamics,"Comput. Methods Appl. Mech. Eng. **100**(1), 63–116 (1992).
[35]M. Dahlby, B. Owren, and T. Yaguchi, "Preserving multiple first integrals by discrete gradients," J. Phys. A: Math. Theor. **44**(30), 305205 (2011).
[36]L. Brugnano, G. Frasca Caccia, and F. Iavernaro, "Energy conservation issues in the numerical solution of the semilinear wave equation," Appl. Math. Comput. **270**(1), 842–870 (2015).
[37]E. Celledoni, V. Grimm, R. I. McLachlan, D. I. McLaren, D. O'Neale, B. Owren, and G. R. W. Quispel, "Preserving energy resp. dissipation in numerical PDEs using the average vector field method," J. Comput. Phys. **231**(20), 6770–6789 (2012).
[38]S. Cray, personal communication, as reported by Joseph E. Flaherty and Stephen F. Davis, July 1989.

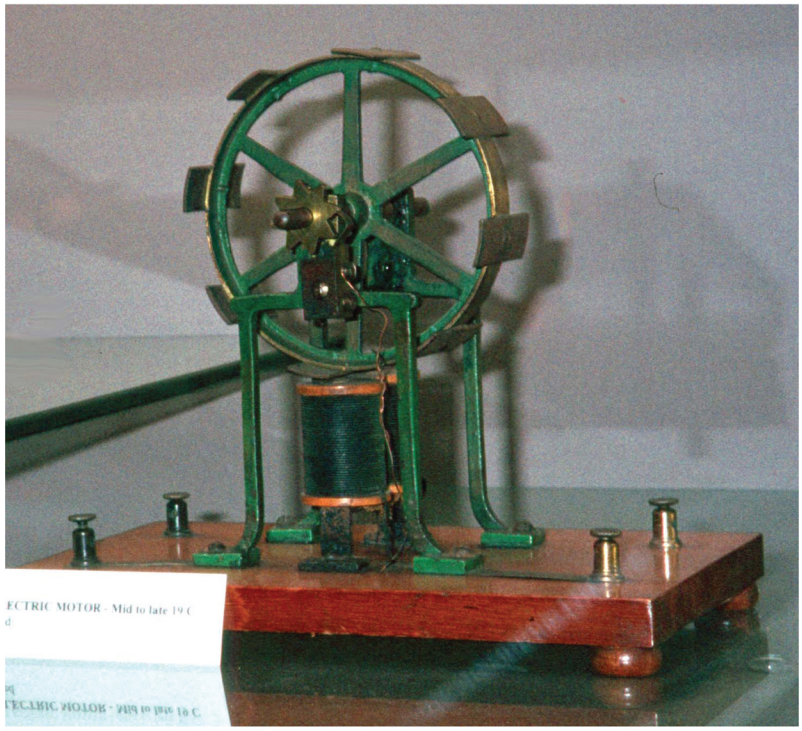

Froment Motor

I photographed this unusual form of electric motor at St. Patrick's College in Maynooth, Ireland in the fall of 1999. It was designed by the French engineer, Paul-Gustav Froment (1815-1865) who in 1844 devised an electric motor that was one of the first used for industrial purposes. In his design, electromagnets are energized to pull in iron bars mounted on a revolving cage. Once the iron bar is level with the electromagnet, the current is cut off until the next iron bar is in range. A commutator is used to make and then break the current to the electromagnet. (Picture and text by Thomas B. Greenslade, Jr., Kenyon College)